Physicochem. Probl. Miner. Process. 53(2), 2017, 1009−1022

www.minproc.pwr.wroc.pl/journal/

Physicochemical Problems of Mineral Processing

ISSN 1643-1049 (print)
ISSN 2084-4735 (online)

Received November 21, 2016; reviewed; accepted February 17, 2017

Comparison of grinding characteristics in high-pressure grinding roller (HPGR) and cone crusher (CC)

Lei Liu[*,,***], Qi Tan[*,**,***], Lu Liu[*,**,***], Wenjun Li[*,**,***], Liang Lv[*,**,***]**

[*] Zhengzhou Institute of Multipurpose Utilization of Mineral Resources CGS, Zhengzhou 450006, China. Corresponding author: tanqibaby@163.com (Qi Tan)
[**] Key Laboratory for Polymetallic Ores' Evaluation and Utilization, MLR, Zhengzhou 450006, China
[***] China National Engineering Research Center for Utilization of Industrial Minerals, Zhengzhou 450006, China

Abstract: We comparatively studied the ball mill grinding characteristics of comminuted hematite products using a high-pressure grinding roll (HPGR) and a conventional cone crusher (CC). The major properties, including grinding kinetics and technical efficiency (E_t), were investigated. The parameters in m-th order grinding kinetics were analyzed, and grinding specific rates were visualized. Ore particles experienced three inherent stages in ball grinding mills, that is *i*) rapid grinding of coarse fraction, *ii*) dynamic grinding of medium size fraction, and *iii*) single grinding of medium size fraction. Particles with size -0.043+0.031 mm were used into dynamic grinding stage earlier than particles -0.105+0.043 mm, and then over-grinding of fines occurred easily. Compared with CC products, HPGR products had significantly shorter turning time points in three breakage stages, implying that HPGR products were ground faster with earlier occurrence of fines over-grinding. HPGR products gave lower E_t at a decreasing rate than the CC products for -2.0 mm and -0.5 mm feeds. Then, it showed a slightly higher value of E_t for -2.0+0.5 mm feed. This indicated that fines over-grinding in HPGR full-size products were more serious under the condition of coarse grinding, whereas the efficiency was higher, and over-grinding weakened significantly in HPGR coarse products because of screening-out fines.

Keywords: *HPGR, grinding kinetics, grinding technical efficiency, ultra-crushing, classified grinding*

Introduction

Comminution, as a prerequisite step for either gravity or flotation separation of valuable minerals from undesired minerals (Gao et al., 2016; Wang et al., 2016), is the most energy-intensive operation in mineral processing. It is estimated that 50% of the energy consumed in US mineral processing plants is used in comminution (Wills and Napier, 2006). As an ultra-fine crushing equipment, the application of the high-pressure grinding roll (HPGR) for industrial comminution has attracted our attention

http://dx.doi.org/10.5277/ppmp170226

because of its low specific energy, low steel consumption, high capacity and high ratio of reduction compared to the conventional tertiary crushers (Schnonert, 1988; Norgate and Weller, 1994; Fuerstenau and Kapur, 1995). HPGR comprises two counter-rotating rolls that draw feed materials into the roll gap. One roll is fixed to the mainframe, while the other movable roll is mounted on slides and positioned by hydraulic rams. The specific pressure (SP) (i.e., total force divided by projected roller area) is typically in the range of 3-9 N/mm^2 depending on different situations, however, pressures up to 1,000 N/mm^2 within the operating gap were also reported (Maxton et al., 2003).

Comminution in HPGR is a result of high inter-particle stresses generated when a bed of solids are compressed while moving down the gap between two pressurized rolls. The priority that HPGR can generate fine products followed by grinding in ball milling, puts a competitive pressure on the application in semi-autogenous (SAG) mills. It is fed from a three-stage crushing system, with HPGR as the third stage. In addition, the possibility of grinding finely at a relatively low energy input and high capacity further expands the use of the technology. Finally, the additional advantages for the downstream processes, such as reducing a work index of the ball mill for subsequent grinding and enhancing leaching performance in gold treatment, make the technology more attractive (Abouzeid and Fuerstenau, 2009; Meer and Gruendken, 2010).

In the former work (Han et al., 2012), we discovered three modes of cracks in HPGR products. Transgranular cracks were originated from shearing breakages. Intragranular and intergranular microcracks were generated by HPGR via two main nonrandom breakage forms, namely preferential breakage and interfacial breakage. It depended on the respective ability to endure stresses when mineral phases (particles) were loaded against each other. The BET values for the same-size fractions showed that HPGR products yielded higher specific surface areas and more pore volumes than jaw crusher products. On this basis, we studied the grinding characteristics of comminuted hematite products using HPGR and conventional CC, as well as major properties like particle size, grinding kinetics and grinding technical efficiency.

Theory

Particle size analysis

A size analysis is of primary importance in determining the quality of comminution and in establishing the degree of liberation of values from the gangue at various particles sizes. The sieve analysis is one of the oldest size analysis methods, accomplished by passing a known weight of sample material through successively finer sieves to determine the percentage weight in each size fraction (Wills and Napier, 2006). The weighted average particle size (D_w) and deviation coefficient (K_d) are calculated by the sieve analysis to describe the fineness and uniformity of products, and the equations are as follows:

$$D_w = \frac{\sum r_i d_i}{\sum r_i} = \frac{\sum r_i d_i}{100} \tag{1}$$

$$K_d = \frac{\sqrt{\sum (d_i - D_w)^2 r_i}}{D_w} \tag{2}$$

where r_i is the weight fraction of material of size i, and d_i the average particle size of the material of size i.

The Rosin-Rammler method is frequently used for representing the results of sieve analyses performed on a material ground in ball mills. Such products were found to obey the following relationship (Wills and Napier, 2006):

$$R = 100 \exp(-bd^n) \tag{3}$$

where R is the cumulative oversize in percent, d the particle size, b and n are constants.

Grinding kinetics

The overall grinding process and the generated size distribution are described by a size-discrete time-continuous population balance model. In this model, milling is expressed in terms of the selection and breakage functions (Austin et al., 1982). On a laboratory scale, the selection and breakage functions are determined by batch grinding tests, which are performed on single particle sizes for a ball charge consisting of a single size. The model equation is given as (Fuerstenau et al., 2010):

$$\frac{dm_i(t)}{dt} = -K_i(t) m_i(t) + \sum_{j=1}^{i-1} K_j(t) b_{i,j} m_j(t) \tag{4}$$

where $m_i(t)$ is the mass fraction of particles in the size interval 'i' at time t (min), $K_i(t)$ is the breakage rate parameter (min^{-1}) for material in the size class 'i' at time t, $b_{i,j}$ is the breakage distribution parameter (unit-less), which gives the fraction of material reporting to size class 'i' when the material in the size class 'j' is comminuted.

Accordingly, $B_{i,j}$ is the cumulative breakage distribution parameter defined as the cumulative mass fraction of material broken from size interval j which appears in size less than the upper size limit of size interval i:

$$B_{i,j} = \sum_{k=1}^{n} b_{k,j} \,. \tag{5}$$

Given that the B parameters must be determined from single size feed grinding data, any likely variation in the B parameters may yield unrealistic K parameters due to grinding environment effect. The difficulty of decoupling the K and B parameters,

as well as the assumption of the compensation condition for the determination of the B parameters by the methods described above, have led researchers to use a cumulative-size basis for the rate of breakage. It does not require a need for the breakage distribution function (Ramirez-Castro and Finch, 1980; Laplante et al., 1987). If this alternative modeling scheme is used with batch ball-mill grinding, or plug flow transport, the grinding model is simplified to (Acar and Hosten, 2013):

$$R_i(t) = R_i(0)\exp(-z_i t^m) \tag{6}$$

where z_i is a constant replacing the breakage rate and distribution parameters as a single breakage parameter, and m corrects for non-first order kinetics.

Equation (6) is changed into Eq. (7) after taking the natural logarithm twice. The plot of $\ln[\ln[R_i(0)/R_i(t)]]$ versus $\ln t$ for linear kinetics should yield a straight line, with the slope and the intercept yielding the parameter m and $\ln z_i$, respectively. (Duan, 1991) found that both pure minerals and actual ores follow the rule that grinding curves are linear in log-log coordinate system:

$$\ln\left[\ln[R_i(0)/R_i(t)]\right] = \ln z_i + m\ln t\,. \tag{7}$$

To study the variation of grinding specific rate (GSR) (v_i), a derivative of Eq. (6) is taken with respect to t, which is stated as follows:

$$v_i = \frac{dR_i(t)}{d(t)} = -R_0 z_i t^{m-1} m\exp(-z_i t^m) \tag{8}$$

where v_i gives GSRs of particles coarser than size i, with units of 1/min, v_i is a vector, with size and direction, $v_i > 0$ reflects the increasing mass percentage of particles coarser than size i as time increases, otherwise, $v_i < 0$ reflects the decreasing mass percentage of particles coarser than size i as time increases. v_i is also described by a size-discrete time-continuous balance model. Size interval grinding specific rates (S_j) after size discretization are the rate difference between the upper limit size and the lower limit size, that is:

$$S_j = v_j - v_{j-1}\,. \tag{9}$$

Grinding technical efficiency

Grinding is a process in which a coarser feed is ground to a specified fineness of x. However, an over-grinding fineness of y should be specified, and the size interval between x and y ($-x+y$) is a suitable size fraction for separation. Considering over-grinding in the grinding process, the grinding technical efficiency (E_t) (Duan, 2012) is the difference-value between total efficiency and over-grinding efficiency, expressed as:

$$E_t = \left(\frac{\gamma - \gamma_1}{100 - \gamma_1} - \frac{\gamma_3 - \gamma_2}{100 - \gamma_2} \right) \tag{10}$$

where $\gamma_1$is the mass fraction of the size fraction finer than x of the feed, γ_2 the mass fraction of the size fraction finer than y of the feed, γ the mass fraction of the size fraction finer than x of the product, γ_3 the mass fraction of the size fraction finer than y of the product.

Experimental

Materials

Hematite samples were taken from Qidashan Mine in China. The samples had d_{50} of 11.2 mm, d_{80} of 18.5 mm, and the moisture less than 0.5%. The raw ores were submitted for mineralogical characterization using a MLA, a software package that is interfaced with a highly automated FEI quanta scanning electron microscope (SEM). Parameters, such as the mineral grain size, mineral locking and mineral associations, mineral constituents, amongst others, were then measured by the system (Vizcarra et al., 2010). Mineral phases of the hematite samples, as determined by MLA, are provided in Tables 1. Iron oxide minerals (including of hematite, magnetite, and limonite) are the valuable minerals, present at ca. 41.49%. Gangue phases are composed primarily of quartz, present at ca. 56.71%. An image of a feed particle is shown in Fig. 1.

Table 1. Raw-ores mineral phases identified by MLA

	Mineral	Mineral weight, %	Mineral	Mineral weight, %
Metallic minerals	Iron oxide ores (Fe_xO_y)	41.49	Ilmenite	0.03
	Pyrite	0.16		
Gangue minerals	Quartz	56.71	Feldspar	0.13
	Chlorite	0.64	Ankerite	0.15
	Dolomite	0.22	Apatite	0.13
	Calcite	0.14	Other	0.20
Total		100.00		

A laboratory-scale CLM-2510 high-pressure grinding roller (HPGR) at Chengdu Leejun Industrial Co., Ltd in China was constructed with two counter-rotating rolls, each 250 mm in diameter and 100 mm in width, with a work gap that can be adjusted from 4 to 9 mm. This fully instrumented mill is powered by two 7.5 kW d.c. motors. The controlling parameter is SPF of 5.2 N/mm^2 and the roll speed is 0.18 m/s. A laboratory-scale cone crusher (CC) at Henan Bailing Machinery Co., Ltd in China is used with a crushing cone of 100 mm in diameter. The CC is powered by a 7.5 kW

d.c. motor, with a max feed size of -30mm and an output adjustment between 2 and 8mm. Hematite samples of 20 kg each were separately crushed by HPGR and CC at once, and then whole products were subjected to screening with 2 mm size. Oversize products were re-crushed with a new feed, and the circulating loads of HPGR and CC at last were 150 and 250%, respectively. The whole undersize products were the finally crushed products after being blended.

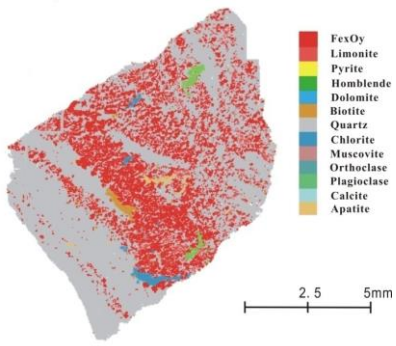

Fig. 1. Image of a feed particle in MLA

Grinding methods

Grinding experiments were performed in a steel mill with the dimension of 140 mm ×160 mm (D×L) and smooth inner surface. The mill was loaded with 3.75 kg ball charge with a size distribution of 25 mm (13 balls), 20 mm (23 balls) and 15 mm (5 balls), as well as running at the speed of 310 rpm. For every test, hematite ores of -2, -2+0.5 and –0.5 mm size fractions of the HPGR and CC products were individually ground in a mass of 300 g, with a solid percentage of 65% (wt.) in the pulp. A full-size distribution of the collected product was obtained using nested screens in decreasing order of size from the top screen down to the 0.031 mm screen.

Results and discussion

Comparison of crushing products size distributions

Compared with CC product, HPGR products had a smaller D_w and a higher K_d (Table 2). This result indicates that HPGR products were finer with a wider size distribution because of a greater proportion of fines (-0.18 mm fraction).

Table 2. D_w and K_d in different crushing products

	HPGR	CC
D_w, mm	0.59	0.75
K_d, %	92.90	73.86

Comparison of grinding kinetics

Figures 2-4 show the *m*-th order plots by different comminution processes. These plots can be described by the *m*-th order grinding kinetics with coefficients of determination R^2 in the range of 0.983 to 0.999 for all the single shapes (Table 3).

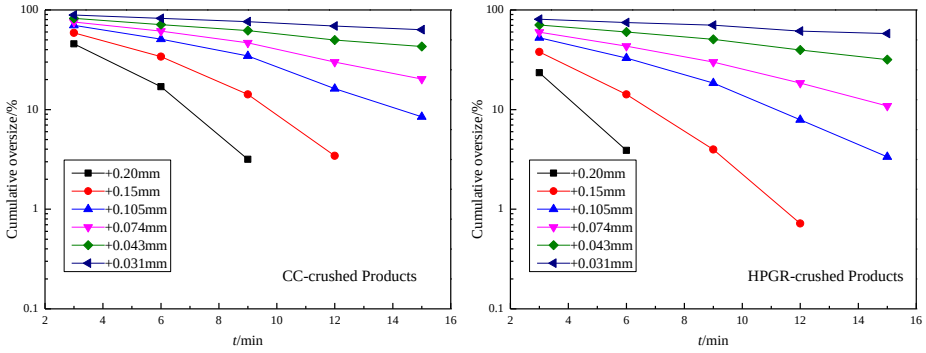

Fig. 2. *m*-th order plots for -2.00 mm feed

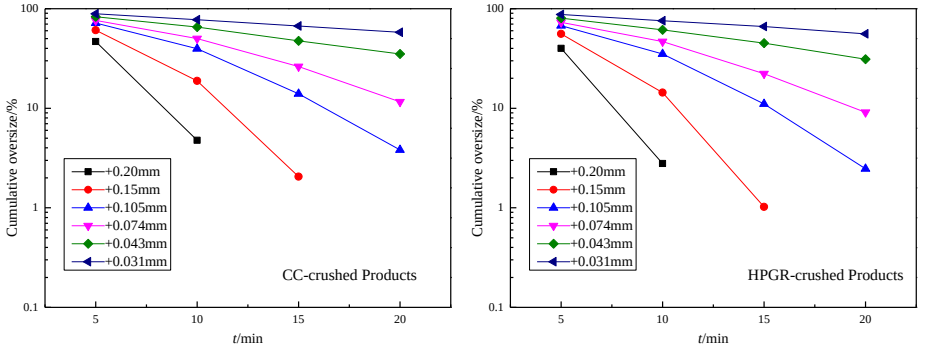

Fig. 3. *m*-th order plots e for -2.0+0.5 mm feed

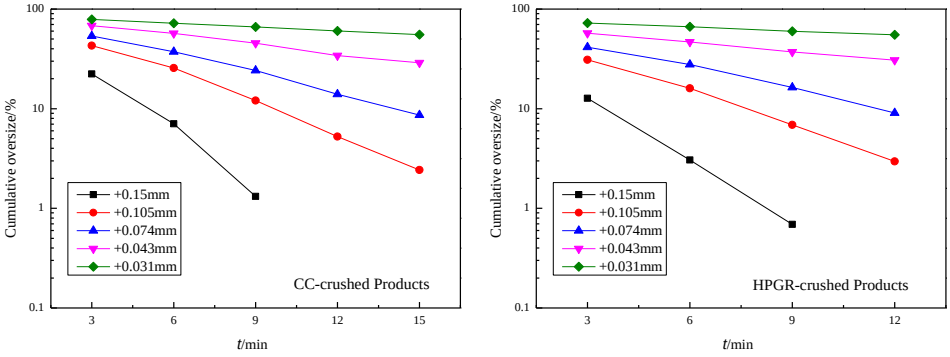

Fig.4 *m*-th order plots for -0.5 mm feed by CC

Table 3. Breakage rate parameters obtained from the laboratory tests

Sieve size, mm	Products	Feed -2.0 mm			Feed -2.0+0.5 mm			Feed -0.5 mm		
		m	z_i	R^2	m	z_i	R^2	m	z_i	R^2
0.20	CC	1.7297	0.0683	0.9987	1.988	0.031	0.998			
	HPGR	1.5329	0.1708	0.9962	1.967	0.038	0.999			
0.15	CC	1.753	0.038	0.997	1.857	0.025	0.998	1.571	0.107	0.999
	HPGR	1.510	0.103	0.999	1.864	0.028	0.999	1.272	0.240	0.999
0.105	CC	1.609	0.028	0.996	1.650	0.023	0.997	1.465	0.061	0.999
	HPGR	1.370	0.073	0.997	1.616	0.028	0.997	1.275	0.119	0.999
0.074	CC	1.502	0.024	0.997	1.489	0.024	0.997	1.418	0.045	0.999
	HPGR	1.265	0.061	0.998	1.458	0.029	0.995	1.278	0.075	0.999
0.043	CC	1.268	0.025	0.998	1.252	0.025	0.999	1.172	0.044	0.997
	HPGR	1.025	0.059	0.993	1.205	0.031	0.999	0.899	0.094	0.999
0.031	CC	1.221	0.015	0.999	1.111	0.020	0.999	1.006	0.029	0.999
	HPGR	0.888	0.039	0.983	1.046	0.025	0.999	0.830	0.050	0.999

The values of v_i can be solved using the m and z_i values in Table 3. Values of S_j for -2.0 mm feed are visualized using a MATLAB software in Figs. 5(a)-(g) (S_j curves for -2.0+0.5 mm feed and -0.5 mm feed are not included because of space limitation, similar to the -2.0 mm curve). The curves of medium j ($0<j<n$) size fraction (including -0.2+0.15, -0.15+0.105, -0.105+0.074, -0.074+0.043 and -0.043+0.031 mm) are in the shape of "inverted, horizontal S" except for the upper limit 0 size fraction (-2.0+0.2mm) and the lower limit n size fraction (-0.031 mm). The curve is from positive to negative and the content of j size fraction decreases after the increase in grinding process. Theoretically, there are two extreme points (t_1 and t_2) in the grinding velocity curve of j size fraction (Figs. 5b and 5c). The grinding process is divided into three stages by two extreme points, which will be described in details.

When grinding time $0 < t \leq t_1$, acceleration $a_j > 0$, and then S_j increases positively. When $t = t_1$, $a_j = 0$, S_j reaches the positive maximum. As to the probability of grinding (P_G), $P_G(<j)$ of $<j$ coarse fraction is much greater than $P_G(j)$ of j size fraction. It is deduced that the content of $\geq j$ fine fraction increases due to rapid grinding of particles of $<j$ coarse fraction, but particles of j size fraction are not effectively ground. It can be regarded as the rapid grinding stage of coarse fraction.

When grinding time $t_1 < t < t_2$, $a_j < 0$, S_j decreases at grinding times longer than t_1 and reaches the maximum negative value at t_2. Particles of j size fraction are effectively ground when $<j$ size fraction continues to be ground. The content of j size fraction entered a process of dynamic change. $P_G(<j)$ decreases with the increase of $P_G(j)$. When $S_j = 0$, $P_G(<j) = P_G(j)$. Meanwhile, the content of j size fraction, reaching dynamic equilibrium point, is the maximum. We set the corresponding time point as t_0. When grinding time $t_1 < t < t_0$, $P_G(<j) > P_G(j)$, and the content of j size fraction

keeps increasing; when grinding time $t_0 < t < t_2$, $P_G(<j)<P_G(j)$, and the content keeps decreasing. When $t = t_2$, acceleration $a_j = 0$, and S_j reaches the negative maximum. At the moment, most of particles of $<j$ coarse fraction are ground, $P_G(j)$ reaches the maximum. It can be regarded as dynamic grinding stage of medium size fraction.

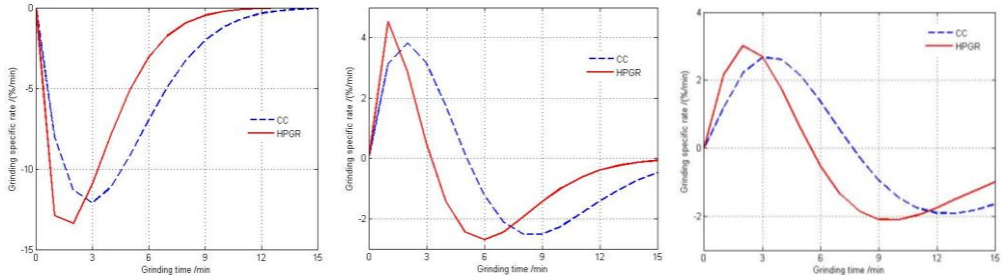

(a) -2+0.2mm fraction (b) -0.20+0.15 mm fraction (c) -0.15+0.105 mm fraction

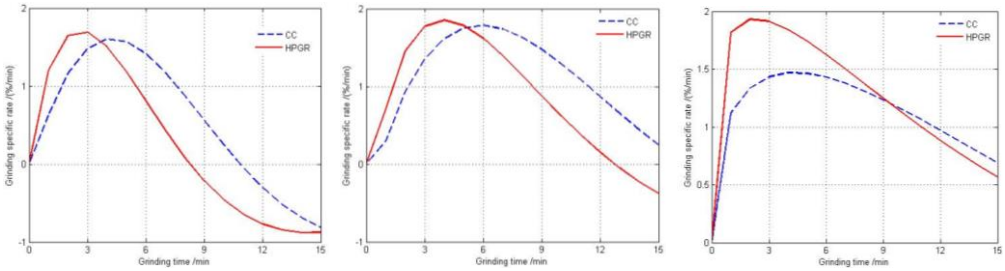

(d) -0.105+0.074 mm fraction (e) -0.074+0.043 mm fraction (f) -0.043+0.031 mm fraction

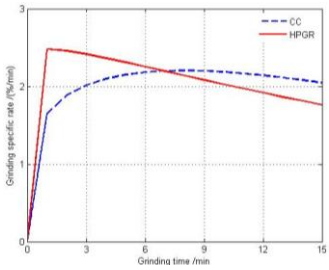

(g) -0.031 mm size fraction

Fig. 5. GSR curves for different fractions

When grinding time $t > t_2$, after $<j$ coarse fraction are ground nearly, j size fraction enters single grinding process, with its increasing amount of 0. The content of j size fraction decreases, and $|S_j|$ gradually declines to 0. It can be regarded as the single grinding stage of medium j size fraction.

Set GSR of different size fractions $S_j = 0$, and acceleration $a_j = 0$, we can obtain t_1, t_2 and t_0 in the breakage rate curve of different crushing products (Table 4).

Figures 5b-5f show products of HPGR and CC as well as three inherent stages in grinding process, that is *i*) rapid grinding of <*j* coarse fraction, *ii*) dynamic grinding of medium *j* size fraction, and *iii*) single grinding of medium *j* size fraction, irrelevant with crushing modes and feed size. Table 4 shows $t_1 << t_2$ of different size fractions. Particles are in the dynamic grinding stage of medium size fraction most of the time in the grinding process, and the content of medium fraction is in the changing dynamic process. With the decline of size fraction range, the time of t_2 and t_0 gradually extends. After extension, the time of t_1 obviously shortens when the size fraction range decreases to -0.043+0.031 mm. It shows that -0.043+0.031 mm size fraction starts to be ground earlier than -0.105+0.043 mm size fraction. Thus, the content of lower limit of size fraction (-0.031 mm) increases rapidly in the early stage, with fines over-grinding.

Table 4. t_1-value, t_2-value and t_0-value in different crushing modes

Feed size, mm	Size, mm	t_1, min		t_2, min		t_0, min	
		HPGR	CC	HPGR	CC	HPGR	CC
-2.0	-2.0+0.2	1.5898	2.8657	-	-	-	-
	-0.2+0.15	0.9719	1.9406	5.9294	8.4707	3.3072	5.0902
	-0.15+0.105	2.1604	3.3544	9.5507	12.5104	5.4895	7.6559
	-0.105+0.074	2.6375	4.2614	14.4352	17.8927*	8.2644	10.8532
	-0.074+0.043	3.9550	5.8858	22.8841*	27.2463*	12.7264	16.3081*
	-0.043+0.031	2.2816	4.3401	43.4871*	43.9422*	22.3935*	24.0035*
	-0.031	1.0134	7.8738	-	-	-	-
-2.0+0.5	-2.0+0.2	3.6891	4.0752	-	-	-	-
	-0.2+0.15	3.0113	3.0267	9.4267	9.7290	6.2789	6.9458
	-0.15+0.105	4.1625	4.3631	13.2983	14.2827	8.8287	9.4232
	-0.105+0.074	4.9696	5.5309	18.6768	20.0486*	11.9527	12.9293
	-0.074+0.043	5.4792	5.9916	27.0823*	28.8741*	16.5153	17.6839
	-0.043+0.031	5.2774	5.7876	49.0556*	50.3540*	27.5351*	28.4673*
	-0.031	0.0009	0.0011	-	-	-	-
-0.5	-0.5+0.1	1.5880	3.1275	-	-	-	-
	-0.1+0.074	1.0197	2.5283	11.2994	13.6484*	3.0652	6.5967
	-0.074+0.031	2.8361	3.9949	27.3822*	28.1563*	13.3850*	14.9518*
	-0.031	≈0	0.0002	-	-	-	-

Note: The data with * in the table are theoretical calculation ones beyond the test time

Furthermore, compared with CC products, t_1, t_2 and t_0 of different size fractions in HPGR products significantly shorten. That is due to presence of micro cracks, HPGR products with faster breakage rate enter dynamic grinding stage of medium size

fraction earlier. Meanwhile, fines over-grinding occur earlier ($t_{1(HPGR)}$=1.0134<< $t_{1(CC)}$=7.8738).

For the given grinding machine under the same grinding conditions, the capacity is inversely proportional to grinding time in the actual production. Namely, the more it is fed, the faster ores go through the grinding machine, with shortened grinding time. Based on the study of grinding dynamics on one hematite ore, the needed grinding time is shorter when ores are crushed with HPGR. Therefore, the residence time of ores in the ball mill can be shortened by increasing the feed rate in actual production. On the one hand, it can improve the processing ability of processing plants. On the other hand, it can reduce the fines over-grinding discharged by the ball mill, thereby improving separation indexes.

Comparison of grinding technical efficiency

The plots presented in Figs. 2-4 can be also described by the Rosin-Rammler equation, with coefficients of determination R^2 in the range of 0.984 to 0.995 for all single shapes:

$$b = f(t) = a_1 x^2 + a_2 x + a_0 \tag{11}$$

$$n = f(t) = c_1 x^2 + c_2 x + c_0 \,. \tag{12}$$

Thus, Eq. (3) is changed to Eq. (13)

$$R = 100\exp[-(a_1 x^2 + a_2 x + a_0) d^{(c_1 x^2 + c_2 x + c_0)}] \tag{13}$$

where a_1, a_2, a_3, c_1, c_2, and c_3 are constants and c_1 is 0 for -2.0+0.5 and -0.5 mm feed.

Size distributions of batch grinding products with grinding times are calculated using Eq. (13), and the parameters are shown in Table 5. In the tests, the E_t and grinding time at different grinding fineness are shown in Figs. 6-8, assuming over-grinding fineness of 0.031 mm.

For -2.0 mm feed and -0.5mm feed (Figs. 7 and 8), HPGR products require considerably shorter grinding time than CC products for the same grinding fineness because of the higher breakage rate, in which time savings are in the range of 2.17 to 3.67 min for -2.0 mm feed, and in the range of 1.48 to 2.09 min for -0.5 mm feed. However, HPGR products yield a lower E_t at a decreasing rate than the CC product, and then two different crushed products have nearly the same E_t at a grinding fineness (-0.074 mm passing 85% for -2.0 mm feed, and -0.074 mm passing 90% for -0.5 mm feed). This result indicates that fine over-grinding in full-size HPGR products is more serious than the CC product (particularly under the condition in a first stage coarse grinding), although the grinding times are markedly shorter.

For the -2.0+0.5 mm feed, as -0.074 mm passing from 45 to 85%, HPGR products also require shorter grinding time than CC products for the same grinding fineness,

and time savings range from 0.75 to 1.03 min. Two products yield similar E_t variation, but HPGR products have slightly higher E_t with an increasing ratio of about 1 percent point. This result indicates that HPGR coarse products have a higher efficiency, and that over-grinding weakens significantly because of the screened-out fines.

Table 5. Parameters of Eq. (13) for different crushing products

Feed size, mm	Products	a_2	a_1	a_0	R^2	c_2	c_1	c_0	R^2
-2.0	CC	0.3794	-1.5463	4.1074	0.999	-0.0018	0.0752	0.6953	0.995
	HPGR	0.2793	2.3647	-4.8329	0.998	-0.0039	0.1119	0.6280	0.997
-2.0+0.5	CC	0.5167	-6.3886	23.1300	0.997	0	0.0359	0.7700	0.999
	HPGR	0.6219	-7.2714	25.1100	0.999	0	0.0391	0.7640	0.993
-0.5	CC	0.5727	-0.8945	9.6039	0.999	0	0.0326	1.0291	0.990
	HPGR	0.9198	-3.3266	18.1510	0.999	0	0.0420	0.9754	0.999

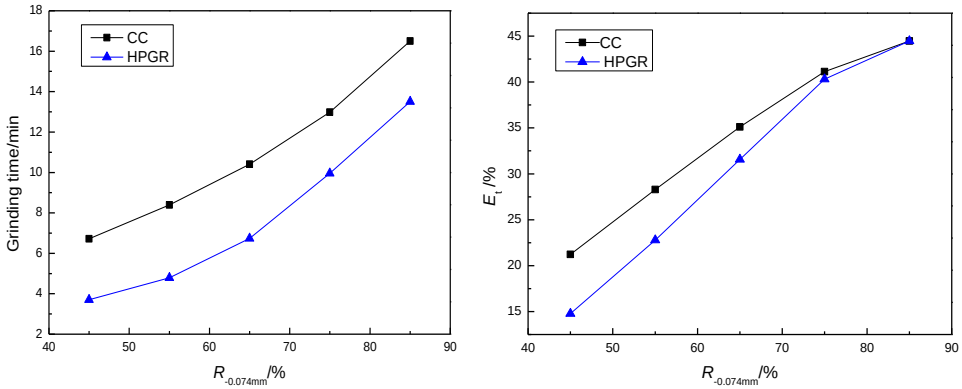

Fig. 6. Variation of grinding time and E_t with grinding fineness for -2.0 mm feed

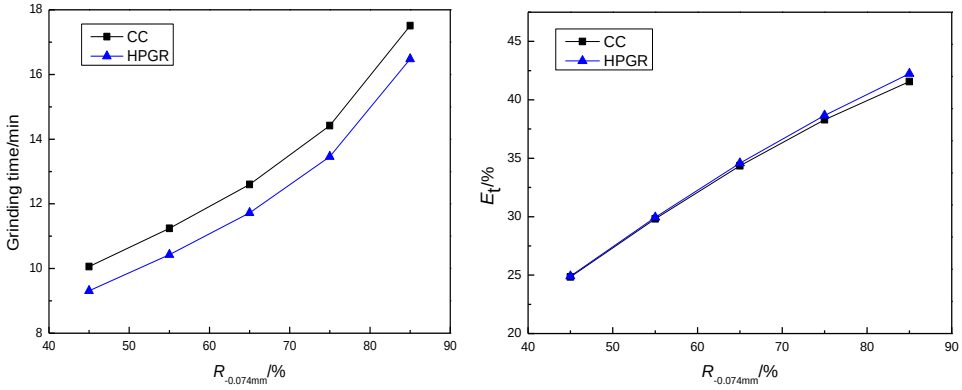

Fig. 7. Variation of grinding time and E_t with grinding fineness for -2.0+0.5 mm feed

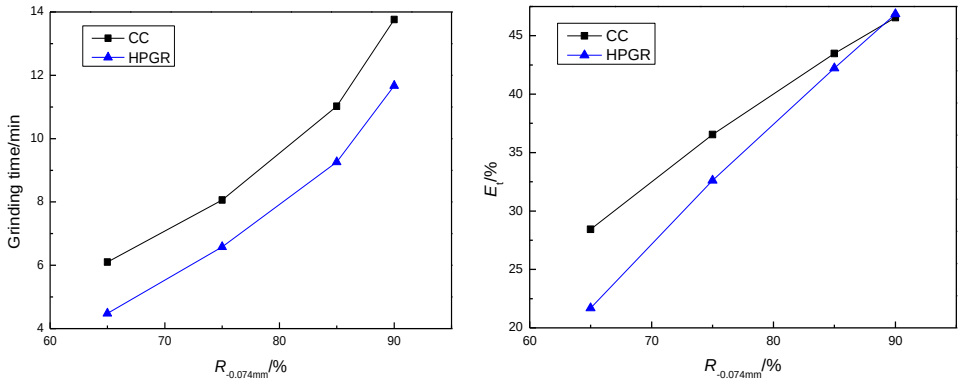

Fig. 8. Variation of grinding time and E_t with grinding fineness for -0.5 mm feed

Conclusions

SFGSR curves showed that ore particles experienced three inherent stages in the grinding process, that is *i*) rapid grinding of coarse fraction, *ii*) dynamic grinding of medium size fraction, and *iii*) single grinding of medium size fraction. Particles in the -0.043+0.031 mm size fraction went into dynamic grinding stage earlier than particles in -0.105+0.043 mm size fraction, and then fines over-grinding occurred easily in the ball mill. Compared with CC products, HPGR products had significantly shorter turning time points in three breakage stages, which proved that HPGR products were ground faster, but fines over-grinding occurred earlier.

The grinding technical efficiency (E_t) was calculated using simulating size distributions of batch grinding products, assuming over-grinding fineness of 0.031 mm. HPGR products required a shorter grinding time than the CC products for the same grinding fineness. As the grinding fineness increased, HPGR products yielded lower E_t at a decreasing rate than the CC product for the -2.0 mm and -0.5 mm feeds, as well as a slightly higher E_t for the -2.0+0.5 mm size fraction feed. These results indicated that fine over-grinding in HPGR full-size products was more serious under the condition of coarse grinding. On the other hand, HPGR coarse products had higher efficiency, and over-grinding weakened significantly because of the screened-out fines.

Acknowledgments

This work was financially supported by the National Natural Science Foundation of China (No.51304175).

References

ABOUZEID, M., FUERSTENAU, W., 2009, *Grinding of mineral mixtures in high-pressure grinding rolls*, International Journal of Mineral Processing 93, 59-65.

ACAR, C., HOSTEN, C, 2013. *Grinding kinetics of steady-state feeds in locked-cycle dry ball milling*, Powder Technology 249, 274-281.

AUSTIN, L. G., SHOJI, K., BELL, D., 1982, *Rate equations for non-linear breakage in mills due to material effects*, Powder Technology 31, 127-133.

DUAN, X. X., 1991, *Selective grinding and its applications*, Metallurgical Industry Press, Beijing, 52.

DUAN, X. X., 2012, *Crushing and grinding (3rd ed.)*, Metallurgical Industry Press, Beijing, 135-136.

FUERSTENAU, D.W., ABOUZEID, A.Z.M., PHATAK, P.B., 2010, *Effect of particulate environment on the kinetics and nergetic of dry ball milling*, International Journal of Mineral Processing 97, 52–58.

FUERSTENAU, D.W., KAPUR, P.C., 1995, *Newer energy-efficient approach to particle production by comminution*, Powder Technology 82, 51-57.

GAO, Y., GAO, Z., SUN, W., HU, Y., 2016, *Selective flotation of scheelite from calcite: A novel reagent scheme*. International Journal of Mineral Processing 154, 10-15.

HAN, Y. X., LIU, L., YUAN, Z. T., WANG, Z., ZHANG, P., 2012, *Comparison of low-grade hematite product characteristics in a high pressure grinding roller and jaw crusher*, Mineral & Metallurgical Processing 29, 75-80.

LAPLANTE, A.R., FINCH, J.A., VILLAR, R. D., 1987, *Simplification of grinding equation for plant simulation*, Trans. Instn. Min. Metall. (Sect. C: Mineral Process. Extr. Metall.) 96, 108-112.

MAXTON, D., MORLEY, C., BEARMAN, R., 2003, *A quantification of the benefits of high pressure rolls crushing in a operating environment*, Minerals Engineering 16, 827-838.

VAN DER MEER, F. P., GRUENDKEN, A., 2010, *Flowsheet considerations for optimal use of high pressure grinding rolls*, Minerals Engineering 23, 663-669.

NORGATE, T.E., WELLER, K.R., 1994, *Selection and operation of high pressure grinding rolls circuits for minimum energy consumption*, Minerals Engineering 7, 1253-1267.

RAMIREZ-CASTRO, J., FINCH, J.A., 1980, *Simulation of a grinding circuit change to reduce lead sliming*, CIM Bull 73, 132-139.

SCHNONERT, K., 1988, *A first survey of grinding with high-compression roller mills*, International Journal of Mineral Processing 22, 401–412.

VIZCARRA, T.G., WIGHTMAN, E.M., JOHNSON, N.W., MANLATIG, E.V., 2010, *The effect of breakage mechanism on the mineral liberation properties of sulphide ores*, Minerals Engineering 23, 374-382.

WANG, J., GAO, Z., GAO, Y., HU, Y., SUN, W., 2016, *Flotation separation of scheelite from calcite using mixed cationic/anionic collectors*. Minerals Engineering 98, 261-263.

WILLS, B. A., NAPIER, T. J., 2006, *Mineral processing technology (Seven Edition)*, Elsevier Science & Technology Books, Queensland, 90, 96-97,146.